2025 IMEKO TC26 International Conference on
Metrology for Archaeology and Cultural Heritage
Bergamo, Italy, October 15-17, 2025

# Multi-Technique Characterization of Mural Paintings at the Santa Maria Gratia Plena Church in Bruzzano Vetere (Calabria, Southern Italy)

Lorenzo Pistorino[1,†,*], Francesco Caridi[1,†,*], Giuseppe Paladini[1], Pasquale Faenza[2], Domenico Majolino[1] and Valentina Venuti[1]

[1] Dipartimento di Scienze Matematiche e Informatiche, Scienze Fisiche e Scienze della Terra, Università degli Studi di Messina, V.le F. Stagno D'Alcontres, 31-98166 Messina, Italy, lorenzo.pistorino@studenti.unime.it (†first author, *corresponding author), fcaridi@unime.it (†first author, *corresponding author) gpaladini@unime.it, dmajolino@unime.it, vvenuti@unime.it
[2]G. Rohlfs Museum of the Calabrian Greek Language, Via Sant'Antonio, 89033, Bova (RC), Italy; pasqualefaenza@yahoo.it

**Abstract – In this study, a multi-technique analytical approach involving X-Ray Fluorescence (XRF) spectroscopy and Micro-Raman Scattering (MRS) was applied to investigate the mural paintings of the Santa Maria Gratia Plena Church, integrated into the medieval fortress of Bruzzano Vetere (Calabria, Italy). The study was aimed at assessing, on one hand, the composition of the pigmenting agents and raw materials used for the realization of the investigated artworks and, on the other hand, at evaluating the degradation processes affecting the painted surfaces and any possible undocumented restoration interventions. The results of such a multidisciplinary approach, which involved the integration of data from different surveys, contribute to a more complete understanding of the state of conservation of the paintings, and offer a scientific basis for future conservation and restoration efforts aimed at preserving and maintaining this historically significant yet currently abandoned site.**

## I. INTRODUCTION

The growing number of publications and specialized scientific conferences demonstrates the increasing recognition of physical techniques as essential tools in archaeometry, offering non-destructive (or minimally invasive) yet highly informative analytical tools for the study and conservation of cultural heritage [1].

Starting from elemental and molecular composition, as achieved by physical analysis, ancient production technologies, processes of alteration and degradation over time, and possible subsequent interventions can be recognized.

In this context, X-Ray Fluorescence (XRF) spectroscopy and Micro-Raman Scattering (MRS) are widely employed as non-invasive physical methods for material characterization, at elemental and molecular scale, respectively [2]. Indeed, their combined application enables enhanced analytical reliability and reduces the need for invasive characterization, thus preserving the integrity of artifacts. Moreover, recent advancements in portable instrumentation have enabled in situ analyses, facilitating studies directly at heritage sites without the need for transportation.

In this paper, XRF and MRS were employed to investigate the mural paintings at the Santa Maria Gratia Plena Church, located in the abandoned village of Bruzzano Vetere (Calabria, Italy). The obtained results contributed to the identification and characterization of the pigments employed, providing crucial insights intended to support future targeted and scientifically informed conservation and restoration strategies, aimed at preserving the artistic and cultural significance of the site.

## II. MATERIALS AND METHODS

### *A. Site description*

The ruins of the Church of Santa Maria Gratia Plena (henceforth referred to as Church) are integrated into the medieval fortress of Bruzzano Vetere, an abandoned village in southern Calabria now part of the metropolitan city of Reggio Calabria (Italy).

Dating back to the 14th century, the Church features a single nave with a projecting apse, a diaconicon and prothesis embedded within the wall [3]. The earliest mention of the Church is recorded in the Apprezzo dello Stato dei Carafa di Bruzzano (1689) [4], although it may be identified with the chiesa *protopale casalis bruzani* cited in 1310 and 1324 [5]. The interior

decoration comprises at least three distinct pictorial phases. The first, dated to the 14th century, is visible in the apse, where two saints are depicted, one of whom has been identified as Saint Basil [6]. The second layer may include the stamped, lanceolate haloes on the northern wall - datable to after the end of the 13th century - and likely associated with saintly figures. The third phase, also visible on the northern wall, consists of twelve rectangular panels featuring saints and a depiction of the Madonna enthroned or enclosed in a mandorla, flanked by angels. This third phase may be dated between the late 14th and the mid-15th century, based on the hairstyle typology of two better-preserved female saints. Subsequent architectural modifications involved the addition of an atrium and the carving of a niche in the northern wall, which led to the partial loss of earlier paintings. The final pictorial layer shows evidence of deliberate abrasion, indicating it was likely completely covered with limewash in the modern period.

### *B. Materials*

A total of 12 samples exhibiting different colorations, i.e. red, dark-blue and yellow, were analyzed in the laboratory, whose description and methods of analysis are reported in Table 1. Micro-fragments, having sizes smaller than ~ 5 $mm^2$, were carefully extracted from the mural paintings, with full respect for the integrity of the archaeological site to ensure minimal impact on the original surface.

*Table 1. List of investigated samples together with a brief description and the employed techniques.*

| Sample | Description | Employed Techniques |
|---|---|---|
| S1 | Red micro-fragment | XRF, MRS |
| S2 | Red micro-fragment | XRF, MRS |
| S3 | Red micro-fragment | XRF, MRS |
| S4 | Red micro-fragment | XRF, MRS |
| S5 | Dark-blue micro-fragment | XRF, MRS |
| S6 | Red micro-fragment | XRF, MRS |
| S7 | Red micro-fragment | XRF, MRS |
| S8 | Dark-blue micro-fragment | XRF, MRS |
| S9 | Red micro-fragment | XRF, MRS |
| S10 | Red micro-fragment | XRF, MRS |
| S11 | Yellow micro-fragment | XRF, MRS |
| S12 | Red micro-fragment | XRF, MRS |

### *C. X-Ray Fluorescence (XRF) measurements*

A portable XRF analyzer (model Alpha 4000, Innov-X Systems) was utilized. The device features a tantalum (Ta) anode X-ray tube and a silicon PIN diode detector with a 170 $mm^2$ active detection area, providing an energy resolution <220 eV at 5.95 keV. It is capable of detecting elements from phosphorus (Z = 15) to lead (Z = 82).

The analysis was performed in "soil" mode with Compton normalization to optimize detection limits. Two consecutive runs were conducted at 40 kV/7 μA and 15 kV/5 μA, with a total acquisition time of 120 seconds. Data acquisition was managed using an HP iPAQ Pocket PC. Instrument calibration was performed using the Light Element Analysis Program (LEAP) II for soil applications and its accuracy was verified using certified reference materials provided by Analytical Reference Materials International.

### D. *Micro-Raman Scattering (MRS) measurements*

Micro-Raman measurements were performed using a portable BTR 111 Mini-RamTM spectrometer (B&W TEK Inc.) equipped with a 785 nm diode laser and a thermoelectrically cooled CCD detector. A BAC151B Raman microscope was used for laser focusing with 40× and 80× objectives, achieving spot sizes of 50 μm and 26 μm, respectively. Spectra were recorded in the range of 60-3150 $cm^{-1}$ with a resolution of 8 $cm^{-1}$. Laser power and acquisition times were optimized to improve the signal-to-noise ratio and reduce fluorescence effects. Multiple scans were accumulated to enhance signal quality, and experimental spectra were compared with reference databases for peak identification [7].

## III. RESULTS AND DISCUSSION

Table 2 reports the elemental composition for all the analyzed samples, as determined through XRF measurements. Furthermore, Fig. 1 provides XRF spectra corresponding to three different fragments, representative of red (S2, Fig. 1a) dark-blue (S5, Fig. 1b) and yellow (S11, Fig. 1c) areas of the mural painting, respectively.

*Table 2. Elemental composition for all investigated samples as obtained through XRF. Minor or trace elements are reported between brackets.*

| Sample | Elemental Composition via XRF |
|---|---|
| S1 | Ca, Fe, S, Sr, Cl (Ar, K) |
| S2 | Ti, Ca, Fe, Sr, (S, K, Mn, Cu, Zn, Rb, Zr, Pb) |
| S3 | Ca, Ti, Fe, Sr, (K, Mn, Zn, Rb, Zr, Pb) |
| S4 | Ca, Ti, Fe, S, Sr, (K, Mn, Zn, Zr) |
| S5 | Ca, Ti, Fe, S, Sr, (Cl, K, Mn, Zn, Br, Sr, Zr, Pb) |
| S6 | Ti, Ca, Fe, Sr, (K, Mn, Zn, Rb, Sr, Zr, Pb) |
| S7 | Ca, Sr, Ti, Fe, (K, Mn, Zn, Br, Rb, Sr, Zr, Pb) |
| S8 | Ti, Ca, Fe (Cl, K, Mn, Zn, Br, Rb, Sr, Zr, Pb) |
| S9 | Ti, Ca, Fe, Sr, (Cl, K, Mn, Zn, Rb, Sr, Zr, Pb) |
| S10 | Ti, Ca, Fe, S, Sr, (Cl, K, Mn, Zn, Br, Rb, Zr, Pb) |
| S11 | Ca, Fe, Ti, (Cl, K, Mn, Zn, Br, Rb, Sr) |
| S12 | Ti, Ca, Fe, (K, Mn, Zn, Br, Rb, Sr, Zr, Mo, Pb) |

All analyzed fragments showed the presence of Ca ($K_\alpha$ and $K_\beta$ transition lines at ~ 3.68 keV and ~ 3.99 keV, respectively) and Fe ($K_\alpha$ and $K_\beta$ at ~ 6.40 keV and ~ 7.05 keV, respectively), indicating a bulk composition

probably made of calcium carbonate ($CaCO_3$) mixed with a Fe-based compound. Furthermore, the occurrence of Ti, detected for all samples with the only exception of sample S1, can be likely related to a Ti-based compound, possibly introduced during modern restoration activities or subsequent handling.

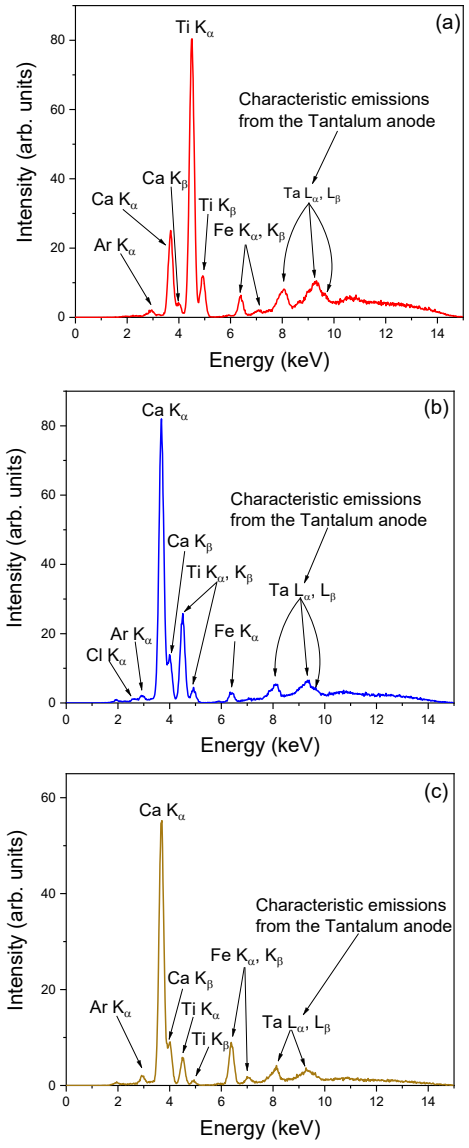


*Fig. 1. XRF spectra, in the 0-15 keV energy range, of red (S2, (a)) dark-blue (S5, (b)) and yellow (S11, (c)) fragments, representative of the corresponding coloured areas of the mural painting.*

In the case of the red-coloured samples (see Fig. 1a for representative spectrum), the absence of Hg and trace levels of Pb suggest that red pigments such as vermilion (HgS) and minium ($Pb_3O_4$) were likely not used. Instead, the detection of characteristic Fe transition lines strongly suggests that the red coloration is attributed to an iron-based mineral from the oxides and hydroxides group, such as hematite ($\alpha$-$Fe_2O_3$), commonly associated with red ochre pigments [7 - 9].

As far as the dark-blue samples are concerned, the elemental composition obtained from XRF (see Fig. 1b) did not provide any chromophoric element typically associated with mineral-based blue pigments, such as Co or Cu. This finding reasonably suggests the possible use of an organic blue pigment of plant and/or animal origin, probably mixed with a carbon-based pigment, such as charcoal and/or bone black ($C+Ca_3(PO_4)_2$), to get the desired dark-blue nuance.

Going on, the high Fe content in the yellow sample, *i.e.* S11 (see Fig 1c), provides strong evidence for the presence of a mineral from the oxides and hydroxides group, most likely goethite ($\alpha$-FeO(OH)), which is widely known as a key component of yellow ochre pigments [7, 8].

Furthermore, with the aim of identifying the molecular composition of all the compounds previously hypothesized through XRF, MRS analyses were carried out. Concerning the red-colored areas of the mural paintings, Fig. 2 shows a photomicrograph and the corresponding micro-Raman spectrum of the representative sample S2 in the 100-2000 $cm^{-1}$ wavenumber range.

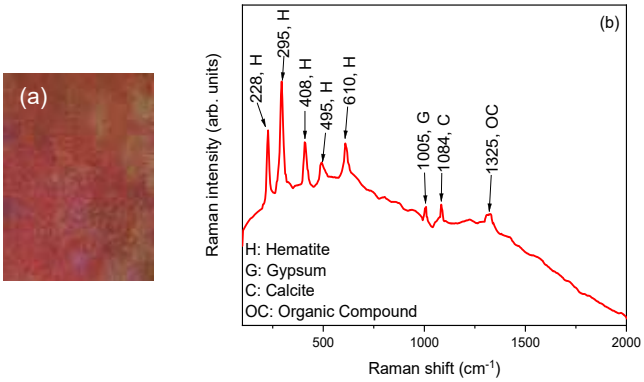


*Fig 2. (a) Photomicrograph in white reflected light of the red micro-fragment S2 and (b) corresponding micro-Raman spectrum, acquired in the 100 - 2000 $cm^{-1}$ range, showing characteristic vibrational peaks attributed to hematite.*

Specifically, bands observed at ~ 228 $cm^{-1}$, ~ 295 $cm^{-1}$, ~ 408 $cm^{-1}$, ~ 495 $cm^{-1}$, and ~ 610 $cm^{-1}$ can be attributed to the presence of hematite ($\alpha$-$Fe_2O_3$), indicating that red ochre was employed for the realization of the red/reddish decorations [2, 7, 10].

Furthermore, besides the presence of hematite, the micro-Raman analysis revealed the presence of gypsum ($CaSO_4$) as indicated by its characteristic peak at ~ 1005

cm$^{-1}$, along with calcite ($CaCO_3$) as evidenced by its distinct band at ~ 1084 cm$^{-1}$. In particular, the presence of gypsum is likely due to degradation processes involving atmospheric sulfur compounds reacting with calcium in the sample. However, its use as a dry painting material, as suggested by Cennino Cennini [12], cannot be ruled out. The author also speaks of a reddish-purple pigment called *caput mortuum*, traditionally produced by calcining yellow ochre with gypsum or kaolin, might be linked to these findings.
As far as the dark-blue areas are concerned, Fig. 3 shows a photomicrograph and the corresponding micro-Raman spectrum of the representative sample S5 in the 100-2000 cm$^{-1}$ wavenumber range.

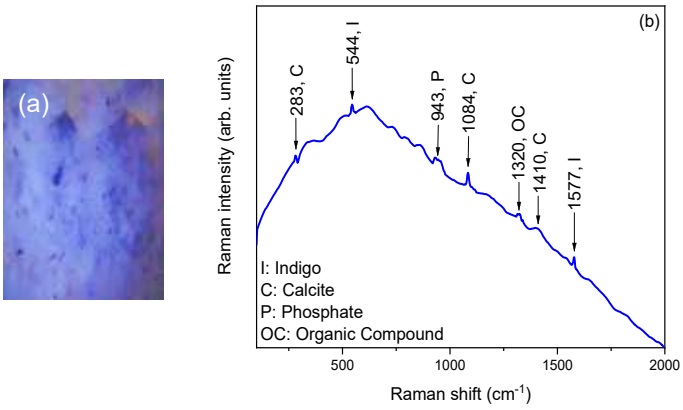


*Fig 3. (a) Photomicrograph in white reflected light of the dark-blue micro-fragment S5 and (b) corresponding micro-Raman spectrum, acquired in the 100 - 2000 cm$^{-1}$ range, showing characteristic vibrational peaks attributed to indigo blue.*

From a first inspection of Fig. 3b, the characteristic bands of indigo blue ($C_{16}H_{10}N_2O_2$), likely derived from *Indigofera tinctoria*, centered at ~ 544 cm$^{-1}$ and ~ 1577 cm$^{-1}$ are detected. In detail, the ~ 544 cm$^{-1}$ band is linked to C-H bending and C-C skeletal vibrations, while the ~ 1577 cm$^{-1}$ spectral feature corresponds to stretching vibrations of conjugated C=C and C=O bonds, as well as N-H bending in the indigo structure [7, 11]. Indigo blue, a deep blue organic compound derived from hydrolysis and oxidation of indican, a glycoside found in plants like *Indigofera tinctoria*, was widely used in Europe since the Middle Age for dyeing textiles, manuscript illumination, and wall paintings. Its use in the Strait of Messina area is documented in a 1292 decree by Frederick III, which restricted its use for dyeing [13, 14].
Going on, the band observed at ~ 1320 cm$^{-1}$ can be related to the Disordered (D) band of amorphous carbon, indicating the presence of carbon black, likely used to darken the color. The presence of bands at ~ 943 cm$^{-1}$, associated with phosphate ($PO_4^{3-}$), and ~ 283 cm$^{-1}$, ~ 1084 cm$^{-1}$ and ~ 1410 cm$^{-1}$ associated with $CO_3^{2-}$ vibrations of calcite, suggests that the pigment is most likely ivory black, traditionally made from charred animal bones [1]. Regarding the yellow areas, Fig. 4 depicts a photomicrograph and the corresponding micro-Raman spectrum of the representative sample S11 in the wavenumber range between 100 and 2000 cm$^{-1}$.

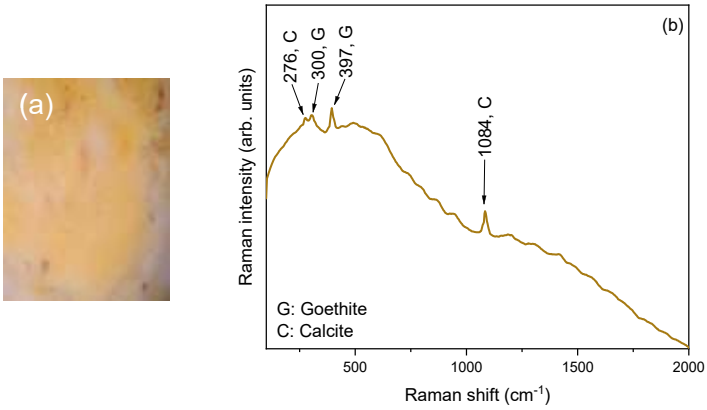


*Fig 4. (a) Photomicrograph in white reflected light of the yellow micro-fragment S11 and (b) corresponding micro-Raman spectrum, acquired in the 100 - 2000 cm$^{-1}$ range, showing characteristic vibrational peaks attributed to goethite.*

The micro-Raman spectrum of the yellow sample exhibits, other than the usual ~ 276 cm$^{-1}$, ~713 cm$^{-1}$ and ~ 1084 cm$^{-1}$ spectral feature ascribed to the presence of calcite ($CaCO_3$), other bands at ~ 300 cm$^{-1}$ and ~ 397 cm$^{-1}$, which can be both attributed to the presence of goethite (α-FeO(OH)), the primary mineral responsible for the yellow ochre coloration, widely employed since prehistoric times in mural paintings, manuscripts, and decorative arts due to its natural abundance, stability, and versatility [2, 7, 15]. This attribution is further supported by the contemporaneous use of goethite-based yellow ochre across Europe during the same period [16].

## IV. CONCLUSIONS

In this study, a multiscale and multi-technique analytical approach was applied to the mural paintings of the Medieval Church of Santa Maria Gratia Plena in Bruzzano Vetere (Calabria, Southern Italy). Through the integration of portable XRF spectroscopy and micro-Raman Scattering (MRS), a comprehensive characterization of the materials used in both the preparatory layers and pigmenting agents was achieved.
As main results, the analysis confirmed the presence of

hematite as the red pigment, indigo blue in the dark blue areas, and goethite as the yellow ochre pigment. Additionally, traces of titanium were found, suggesting possible modern interventions or environmental contamination. The presence of gypsum was detected as well, likely resulting from either dry painting techniques or degradation due to exposure to atmospheric agents, considering the deteriorated state of the site.

In conclusion, it is worth noting that the study is based on a limited set of 12 micro-samples, selected to represent the main chromatic areas. Although surface alteration phenomena may have locally influenced the spectroscopic response, these findings provide insights into the historical material used and offer a foundation for the development of novel conservation strategies aimed at preserving the site's cultural significance.

REFERENCES


[1] Caridi, F., Ricca, M., Paladini, G., Crupi, V., Majolino, D., Donato, A., & Venuti, V. (2022). Multi-technique diagnostic investigation in view of the restoration of *The Glory of St. Barbara* painting by Mattia Preti. *Applied Sciences*, 12, 1385.

[2] Bersani, D., & Lottici, P. P. (2016). Raman spectroscopy of minerals and mineral pigments in archaeometry. *Journal of Raman Spectroscopy*, 47, 499 - 530.

[3] Minuto, D. (1977). *Catalogo dei monasteri e luoghi di culto tra Reggio e Locri* (p. 264). Roma, Italy.

[4] Laganà, C. (2013). *Apprezzo dello "stato" dei Carafa di Bruzzano, anno 1689*. Locri, Italy.

[5] Vendola, D. (1939). *Rationes decimarum Italiae nei secoli XIII e XIV. Apulia-Lucania-Calabria* (pp. 237, 250). Città del Vaticano.

[6]Riccardi, L. (2021). *Corpus della pittura monumentale bizantina. Calabria II* (p. 203). Soveria Mannelli, Italy.

[7] Pigments Checker – Modern & Contemporary Art. (2025, May 10). CHSOS. http://chsopensource.org/tools-2/pigments-checker/

[8] Lafuente, B., Downs, R. T., Yang, H., Stone, N., Armbruster, T., & Danisi, R. M. (2015). The power of databases: The RRUFF project. *Highlights in Mineralogical Crystallography*, 1, 25.

[9] D'Amico, S., Comite, V., Paladini, G., Ricca, M., Colica, E., Galone, L., & Venuti, V. (2021). Multitechnique diagnostic analysis and 3D surveying prior to the restoration of *St. Michael Defeating Evil* painting by Mattia Preti. *Environmental Science and Pollution Research*, 1–20.

[10] Mastrotheodoros, G. P., & Beltsios, K. G. (2022). Pigments—Iron-based red, yellow, and brown ochres. *Archaeological and Anthropological Sciences*, 14(2), 35.

[11] Castro, K., Vandenabeele, P., Rodríguez-Laso, M. D., Moens, L., & Madariaga, J. M. (2004). Micro-Raman analysis of coloured lithographs. *Analytical and Bioanalytical Chemistry*, 379, 674–683.

[12] Tamboni, G. (1821). *Di Cennino Cennini. Trattato della pittura* (pp. 49, 72). Roma, Italy.

[13] Caggese, R. (1922). *Roberto d'Angiò e i suoi tempi* (Vol. I, p. 301). Firenze, Italy.

[14] Cavigli, R. (2021). Il restauro della Croce dipinta di Cortona. *Accademia Etrusca di Cortona*, 88(II), 167–176.

[15] Briani, F., Caridi, F., Ferella, F., Gueli, A. M., Marchegiani, F., Nisi, S., & Venuti, V. (2023). Multi-technique characterization of painting drawings of the pictorial cycle at the San Panfilo Church in Tornimparte (AQ). *Applied Sciences*, 13, 6492.

[16] Hradil, D., Grygar, T., Hradilová, J., & Bezdička, P. (2003). Clay and iron oxide pigments in the history of painting. *Applied Clay Science*, 22(5), 223–236.